ASTRONOMY
AND
ASTROPHYSICS

ASCA and other contemporaneous observations of the blazar B2 1308+326

D. Watson[1], **N. Smith**[2], **L. Hanlon**[1], **B. McBreen**[1], **F. Quilligan**[1], **M. Tashiro**[3], **L. Metcalfe**[4], **P. Doyle**[5], **H. Teräsranta**[6], **A. Carramiñana**[7], and **J. Guichard**[7]

[1] Department of Experimental Physics, University College Dublin, Belfield, Dublin 4, Ireland
[2] Department of Applied Physics and Instrumentation, Cork Institute of Technology, Cork, Ireland
[3] Department of Physics, University of Tokyo, Hongo, Bunkyo-ku, Tokyo, 113-0033, Japan
[4] ISO Data Centre, Astrophysics Division, Space Science Department of ESA, Villafranca del Castillo, P.O. Box 50727, 28080 Madrid, Spain
[5] Physics Department, National University of Ireland, Cork, Ireland
[6] Metsähovi Radio Observatory, 02540 Kylmälä, Finland
[7] Instituto Nacional de Astrofísica Optica y Electrónica, Luis Enrique Erro 1, Tonantzintla, Puebla 72840, México

Abstract. The high redshift ($z = 0.997$) blazar B2 1308+326 was observed contemporaneously at x-ray, optical and radio wavelengths in June 1996. The x-ray observations were performed with ASCA. The ASCA results were found to be consistent with reanalysed data from two earlier ROSAT observations. The combined ASCA and ROSAT data reveal an x-ray spectrum that is best fit by a broken power law with absorber model with photon spectral indices of $\Gamma_{\mathrm{soft}} = 3.4^{+5.1}_{-1.1}$ and $\Gamma_{\mathrm{hard}} = 1.63^{+0.10}_{-0.09}$ and a break energy at $1.1^{+0.4}_{-0.4}$ keV in the rest-frame of the blazar. The break in the x-ray spectrum is interpreted, from the shape of the simultaneous broadband spectral energy distribution, to be the emerging importance of inverse Compton (IC) emission which dominates the ASCA spectrum. The faint optical state reported for these observations ($m_V = 18.3 \pm 0.25$) is incompatible with the high synchrotron flux previously detected by ROSAT. The IC emission detected by both ROSAT and ASCA was not significantly affected by the large change in the synchrotron component.

Mg II emission was detected with an equivalent width (W_λ) of ~ 15 Å, significantly different from previously reported values. The small and variable W_λ in B2 1308+326 may be due to the highly variable continuum and not intrinsically weak lines in the source. A lower limit on the Doppler boost factor calculated from the contemporaneous data is consistent with expectations for highly polarised quasars and higher than expected for BL Lacs. Absorption at a level of $N_H = 3.0^{+2.3}_{-0.6} \times 10^{20}$ cm^{-2} was detected which is in excess of the Galactic value of $N_H = 1.1 \times 10^{20}$ cm^{-2}, indicating the possible presence of a foreground absorber. A gravitational microlensing scenario cannot therefore be ruled out for this blazar. No significant variability on timescales of hours was detected in the optical or x-ray data.

B2 1308+326 could be a typical radio-selected BL Lac in terms of peak synchrotron frequency and optical and radio variability but its high bolometric luminosity, variable line emission and high Doppler boost factor make it appear more like a quasar

than a BL Lac. It is suggested that B2 1308+326 be considered as the prototype of this class of composite source.

1. Introduction

The classification of the high redshift ($z = 0.997$) source B2 1308+326 is uncertain (Gabuzda et al., 1993). It has been designated a BL Lac (Stickel et al., 1991) because of its almost featureless optical spectrum (Wills & Wills, 1979), its strong optical variability (Mufson et al., 1985) and the high degree of polarization of its optical continuum (Angel & Stockman, 1980). As one of the 1 Jy sample of BL Lacs, B2 1308+326 is classified as a Radio-Selected BL Lac (RBL) (Stickel et al., 1993).

However, B2 1308+326 also exhibits quasar-like properties. VLBI polarisation images show that the polarised flux from the inner part of the jet is nearly perpendicular to the direction of the jet which is a characteristic property of quasars not BL Lacs (Gabuzda et al., 1993). The degree of core polarisation from VLBI observations of B2 1308+326 is somewhat higher than usual for quasars and at the lower end of the range for BL Lacs (Gabuzda et al., 1993). Measurements of the apparent speed of knots emerging from the core are superluminal ($3.6h^{-1}c$, $8h^{-1}c$, $21h^{-1}c$) and above the typical speeds observed in BL Lacs (Gabuzda et al., 1993). B2 1308+326 also shows an optical-UV excess above the IR extrapolation (Brown et al., 1989), and its radio power and morphology are FR II (Fanaroff & Riley, 1974, type II) in nature (Kollgaard et al., 1992). The FR II classification is not that unusual among BL Lacs (Kollgaard et al., 1996), but an FR I morphology would strongly militate against its being a quasar (Urry et al., 2000; Kollgaard

et al., 1990). The large bolometric (Sambruna et al., 1996) and 5 GHz luminosities (Kollgaard et al., 1992) are further indications that it could be regarded as a quasar. The term "blazar" is particularly useful for sources like this, encompassing as it does flat spectrum radio quasars (FSRQs) and BL Lacs. It must be noted that the terms highly polarised quasars (HPQs), optically violently variable (OVV) quasars, FSRQs (and more recently, quasar-hosted blazar) are used to refer to blazar subclasses. The significant distinction here is between quasar-type and BL Lac-type blazars and the term FSRQ is used except in cases where another classification occurs in a work cited in the text.

Two main approaches have proven to be effective in constraining models of BL Lacs; monitoring their variability (e.g. Georganopoulos & Marscher 1998a), and studying their broadband spectral energy distributions (SEDs) (e.g. Sambruna et al. 1996, Kubo et al. 1998, Sambruna et al. 1999). Rapid flux variations and changes in the shape of the SEDs of blazars are common (e.g. Pian et al. 1998, Macomb et al. 1995, Chiaberge & Ghisellini 1999). To place adequate constraints on the synchrotron emission (e.g. the Doppler boost factor of the putative jet and the angle between such a jet and the line of sight) in these sources requires simultaneous observations over a wide range of frequencies.

It has been suggested that some sources with BL Lac characteristics are actually gravitationally microlensed quasars (Nottale, 1986; Ostriker & Vietri, 1990). The best candidates include AO 0235+164 (Rabbette et al., 1996), PKS 0537-441 (Romero et al., 1999) and MS 0205.7+3509 (Watson et al., 1999). B2 1308+326 has characteristics intermediate between BL Lacs and quasars. Gabuzda et al. (1993) have therefore suggested that B2 1308+326 may be gravitationally microlensed. Observation of a foreground galaxy would lend support to the argument that it is indeed gravitationally lensed. However high resolution imaging with the HST WFPC2 (Urry et al., 1999) did not confirm the detection of spatially extended emission reported by Stickel et al. (1993). The observations were consistent with a point source with an upper limit of $m_I \geq 26$ mag arcsec^{-2} for any surrounding galaxy.

In the superluminal micro-lensing scenario, the time scale for rapid variability can constrain source parameters (e.g. Lorentz factor and source diameter, McBreen & Metcalfe 1987, Gopal-Krishna & Subramanian 1991). Such microlensing variations should be achromatic and therefore detectable with simultaneous multi-wavelength observations.

Simultaneous x-ray, optical and radio observations were carried out in order to constrain the nature of the emission in B2 1308+326. These observations and the data reduction procedures are described in Sect. 2. Results are presented in Sects. 3 and 4 and are discussed in Sect. 5 with conclusions in Sect. 6. $H_0 = 75$ km s^{-1} Mpc^{-1} and $q_0 = 0.5$ are assumed throughout.

2. Observations and data reduction

2.1. X-ray observations

Observations of B2 1308+326 were made with the ASCA satellite (Tanaka et al., 1994) between 15:26 and 23:41 UT on 10 June 1996, and between 23:37 UT on 11 June 1996 and 09:10 UT on 12 June 1996. There are four instruments on board ASCA, two Gas Imaging Spectrometers (GIS-S2 and GIS-S3) and two Solid-state Imaging Spectrometers (SIS-S0 and SIS-S1). The instruments have a well-calibrated energy range of 0.7–10.0 keV for the GIS and 0.5–10.0 keV for the SIS and only data in these energy ranges were used for spectral fitting. The total exposure time per instrument was approximately 40 ks. The SIS data were recorded in FAINT data mode and converted to BRIGHT-2 mode (Inoue, 1993) having corrected for the Residual Dark Distribution (RDD) effect with the FTOOLS script 'Correctrdd'.

Data from the SIS and GIS instruments were screened in a standard way, and were then reduced using the FTOOLS applications. An extraction region was defined around the source, with an aperture of 4′ for the SIS detectors and 6′ for the GIS. This spatial region was used to extract the source plus background counts. An estimate of the background was derived by taking an annulus around the extraction aperture and extracting counts from this region. An alternative background estimate was derived from separate dark-sky observations made by ASCA and results obtained using both types of background estimates were found to be consistent. The annulus background was subtracted from the extracted source plus background counts to obtain a source spectrum. The resulting spectra were rebinned to have a minimum of 20 counts per bin in order to ensure the validity of the Gaussian approximation.

Two observations of the source were made with the ROSAT PSPC (Pfeffermann & Briel, 1986) on 23 June 1991 (Comastri et al., 1995; Lamer et al., 1996) and 3 June 1992. These data were reduced in a standard way using the FTOOLS software. The response matrix from ROSAT AO-1 was used to analyse the data from the 23 June 1991 observation, and that from AO-2 for the 3 June 1992 observation. Only the well-calibrated data between 0.1–2.4 keV were used.

2.2. Optical and radio observations

Optical Johnson V-band observations were carried out under photometric conditions with the 1.23 m telescope at Calar Alto Observatory, Spain on the nights of 10 and 11 June 1996 with typical exposure times of 900 s. Standard CCD aperture photometry techniques were used to reduce the data. Absolute calibration of the source was derived using V-band differential photometry on a calibrated reference star within the CCD field of view (star C from Fiorucci et al. 1998). Optical V-band observations made two weeks later with the 1 m JKT telescope at La Palma Observatory showed the source to be of the same magnitude, within the error of 0.25 mag. The relative uncertainty (0.08 mag.) in the optical magnitude was brought below the absolute calibration uncertainty (0.25 mag.), by using differential photometry techniques (Rabbette et al., 1998).

Observations were carried out under non-photometric conditions at the 2.12 m telescope of the Observatorio "Guillermo Haro" at Cananea, Son., México on June 16, 1996 using the Landessternwarte Faint Object Spectrograph and Camera (LFOSC) in ∼5.5 Å/pixel mode. The standard IRAF utility package dis-

Table 1. Comparison of fits (using model A, a simple power-law plus absorber) to data from: each ASCA detector individually (S0, S1, S2, S3), from the combined ASCA detectors (A), from the ROSAT observations of 23 June 1991 (R1) and 3 June 1992 (R2) and from both ASCA and ROSAT, fit simultaneously (A+R). N_H is the equivalent hydrogen column, Γ is the photon index, F_{1keV} is the flux in photons/keV/cm^2 s^{-1} at 1 keV, χ^2/DOF is the value of χ^2 for that fit with DOF degrees of freedom and N. H. Prob. is the probability of the χ^2 obtained being at least as large as it is if the data come from a parent distribution described by the model. Ranges in parentheses are 90% confidence intervals for 1 parameter of interest.

	N_H $(10^{20} cm^{-2})$	Γ	F_{1keV} $(\times 10^{-4})$	χ^2/DOF N. H. Prob.
S0	0.0	1.45	1.94	46/45
	(0.0–11.6)	(1.28–1.71)	(1.67–2.55)	0.45
S1	0.4	1.38	1.82	29/38
	(0.0–14.6)	(1.18–1.74)	(1.52–2.60)	0.84
S2	24.5	2.21	2.94	37/49
	(0.0–102.4)	(1.59–3.24)	(0–9.20)	0.90
S3	0.0	1.83	2.42	67/61
	(0.0–22.3)	(1.52–2.23)	(1.82–3.59)	0.27
A	0.0	1.75	1.99	205/202
	(0.0–2.5)	(1.66–1.84)	(1.87–2.16)	0.43
R1	1.35	2.01	2.19	34/30
	(0.84–1.94)	(1.76–2.27)	(1.99–2.39)	0.29
R2	0.81	1.75	1.89	10/12
	(0.00–2.15)	(1.29–2.30)	(1.61–2.17)	0.66
A+R	1.36	1.88	2.15	250/247
	(1.14–1.58)	(1.80–1.96)	(2.05–2.25)	0.43

Table 2. Results from best-fit broken power-law plus absorber model (B), to data from different observations; R1 and R2 are the ROSAT observations of 23 June 1991 and 3 June 1992 respectively; A represents the simultaneous fit to the data from the ASCA observations of 10–12 June 1996; A+R is a simultaneous fit to all the ROSAT and ASCA data. Ranges in parentheses are 90% confidence intervals for 1 parameter of interest. $\Gamma 1$ and $\Gamma 2$ are the photon spectral indices below and above the break energy respectively.

	N_H $(10^{20} cm^{-2})$	$\Gamma 1$ (soft)	Break (keV)	$\Gamma 2$ (hard)
R1	8.4	≥ 10.0	0.38	2.1
	(6.35–8.69)	(3.04–)	(0.35–0.43)	(1.7–2.4)
[a]R2	7.1	10.0	0.33	2.32
	(5.1–7.6)	(–)	(0.28–0.42)	(1.58–2.49)
[a]A	2.78	10.0	0.45	1.62
	(0.0–9.7)	(–)	(0.21–0.56)	(1.54–1.77)
A+R	3.0	3.4	0.57	1.63
	(2.4–5.3)	(2.3–8.5)	(0.36–0.77)	(1.54–1.73)

[a] $\Gamma 1$ is unconstrained for the ASCA and R2 data, since model B is not a significantly better fit than model A for these data alone (see Table 3).

Table 3. Fit comparisons for models A, power-law plus absorber and B, broken power-law plus absorber. N. H. Prob. is the probability of the χ^2 obtained being at least as large as it is if the data come from a parent distribution described by the model. The f-test Prob. refers to the probability derived from the f-test of the hypothesis that an additional component (i.e. spectral break) yields an improved description of the data. R1 and R2 are the ROSAT observations of 23 June 1991 and 3 June 1992 respectively; A represents the ASCA observations of 10–12 June 1996; A+R is a simultaneous fit to all the ROSAT and ASCA data. The spectral break is not significant in the ASCA or R2 data individually, but is significant in R1 alone and in the A+R simultaneous fit.

Obs.	A: abs×pow N.H. Prob.	$\frac{\chi^2}{DOF}$	B: abs×bknpow N.H. Prob.	$\frac{\chi^2}{DOF}$	f-test Prob.
R1	0.286	34/30	0.707	24/28	0.994
R2	0.657	10/12	0.657	7.7/10	0.651
A	0.431	205/202	0.433	203/200	0.645
A+R	0.430	250/247	0.621	238/245	0.998

tributed by the National Optical Astronomy Observatories was used to reduce the data. The spectral images were processed to obtain one-dimensional spectra of the object and the sky by co-adding the counts on each channel along the slit, through user defined apertures.

The wavelength calibration was performed using the identified lines of the comparison arcs in order to obtain a dispersion solution. With the derived coefficients the wavelength calibration of the spectra was then carried out. Due to the non-photometric conditions during these spectral observations, the spectrophotometric calibration proved to be unreliable.

The results of radio observations at 22 GHz and 37 GHz performed at the Metsähovi Radio Observatory, Finland for the period 1980–2000 are included here. The observing and data reduction procedures are described in Teräsranta et al. (1998).

3. X-ray spectral fits

The x-ray data from both ASCA observations were compared for variability above a significance level of 2σ. No variability was detected and the data were therefore coadded per detector for further analysis.

Data from the four ASCA instruments were fit individually using the Levenberg-Marquardt algorithm in XSPEC. Model A, a power-law with an absorber as defined by Morrison & Mc-

Cammon (1983) was fit to these data and yielded acceptable fits and consistent results (Table 1).

Since the ASCA instruments showed no significant spectral differences, the binned spectra from all four detectors were fit simultaneously. The data were fit to model A (Table 1) and to model B, a broken power-law with absorber (Table 2). The f-test (Bevington & Robinson, 1992) was applied to models A and B to establish whether the fit was significantly improved by the addition of the two extra terms in model B (Table 3). Model B did not yield a significant improvement over model A in the fit to the ASCA data alone (Table 3).

The ROSAT data from 23 June 1991 were published by Comastri et al. (1995). The results of a single power-law with absorber fit (model A) to this ROSAT data were found to be compatible with and had a similar reduced χ^2 statistic, χ^2_ν (Table 1) to that obtained by Comastri et al. (1995) for the same
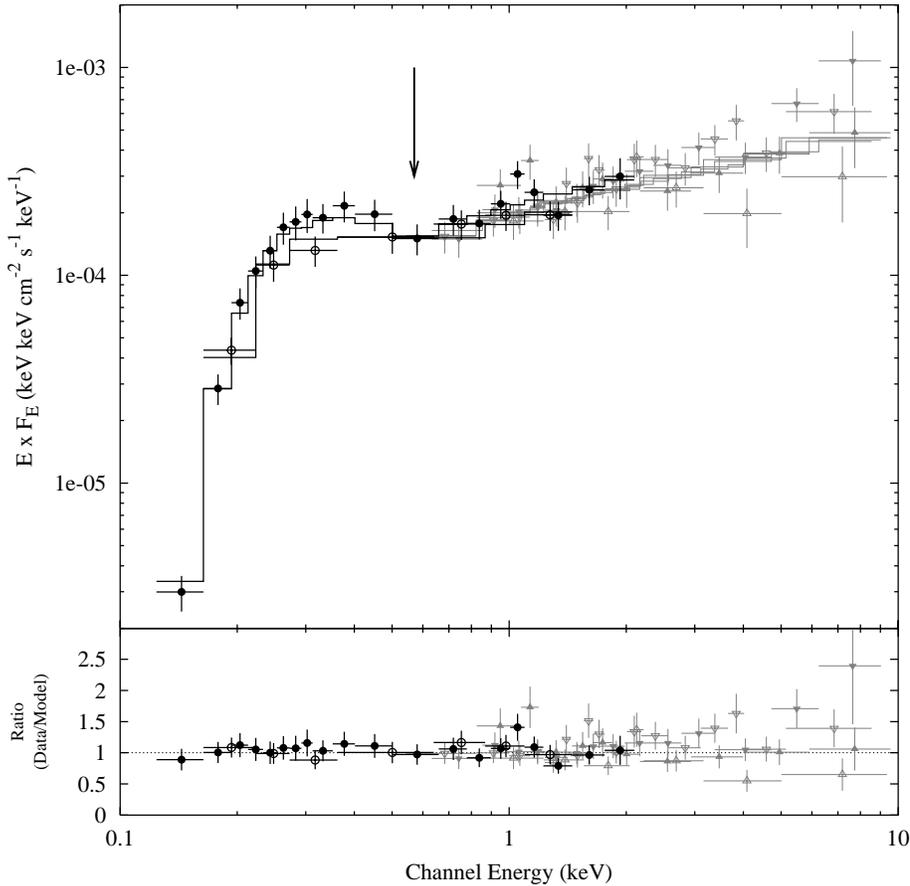
Fig. 1. Best fit (observer frame) $E \times F_E$ spectrum to joint ASCA and ROSAT data with data/model ratio. The break at 0.57 keV is indicated. Data from the ASCA instruments are plotted in grey (S0 '▽', S1 '▼', S2 '△' and S3 '▲'). ROSAT observations are plotted in black (R1 (23 June 1991) '•', R2 (3 June 1992) '○'.)

data and model. Although model A provides an acceptable fit ($\chi^2_\nu = 1.13$) to the ROSAT data of 23 June 1991 (R1), the f-test indicates that a broken power-law is a significantly better fit (Table 3). The spectral break is clearly detected in this data alone (Fig. 1). Data from the ROSAT observation of 3 June 1992 (R2) is acceptably fit by model A; there is no significant improvement in the fit to this data using model B (Table 3).

The energy of the spectral break is at the low energy end of the SIS detector range and outside that of the GIS. The ROSAT observation of 3 June 1992 unfortunately does not constrain the models very well. It is not surprising therefore that there is no significant improvement in the fit for either of these observations using a broken power-law model. Data from both ROSAT observations were fit with model B and the results were found to be consistent with the results from the fit of model B to the ASCA data (Table 2). No variation was found at the level of 95% significance, in the 0.5–2.4 keV flux between any of the observations.

The consistent results indicate that the x-ray spectrum had not altered substantially between the ROSAT and ASCA observations (see the next section for further discussion on this point). The combined ROSAT and ASCA data were therefore fit simultaneously, allowing the normalization parameter to vary independently between the two ROSAT observations and the combined ASCA data, but constraining the other parameters to be the single best-fit for all datasets. The flux normalizations

were left free to vary independently to allow for any residual systematic differences between the instruments.

Model B was the best fitting model to the combined ASCA and ROSAT data and was used for all further analysis. Although a discrepancy of $\Delta\Gamma \sim 0.4$ has been noted in the spectral indices reported for observations with ASCA SIS and ROSAT PSPC (Iwasawa et al., 1999), the detection of the spectral break does not depend on differences between the ROSAT and ASCA spectral indices since the break is clearly detected in the R1 data alone. The results of a comparison between models A and B for all the x-ray observations are summarised in Table 3.

4. Results

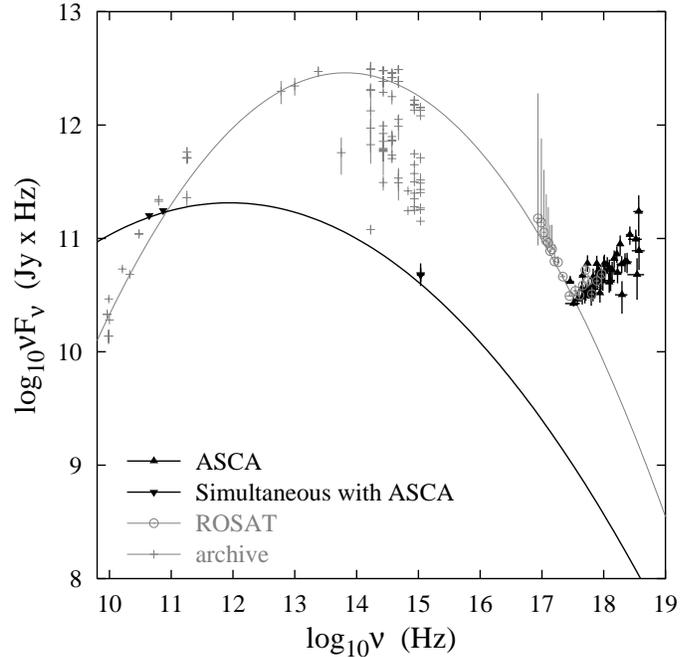The deconvolved data from all instruments with the best-fit model and the data/model ratio are plotted in Fig. 1.

Confidence contours for the best-fit model for the two parameters of interest, equivalent Hydrogen absorbing column (N_H) and the spectral break energy, are shown in Fig. 2. The soft x-ray absorption at 3.0×10^{20} cm^{-2} is above the Galactic level of 1.1×10^{20} cm^{-2} given by Dickey & Lockman (1990).

The rest-frame SED is plotted in Fig. 3. The break in the ROSAT spectrum is clearly evident at 1.1 keV (2.8×10^{17} Hz). It is generally accepted that the two broad emission components that characterise blazar SEDs are due to synchrotron emission at lower energies and inverse Compton (IC) emission at higher energies (Costamante et al., 2000; Fossati et al.,
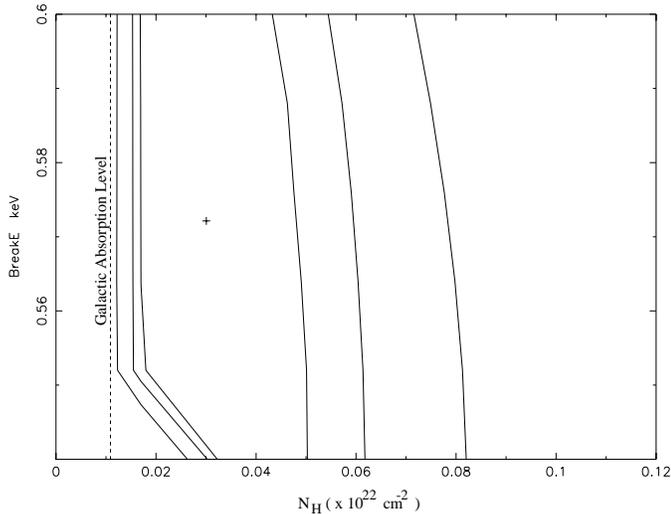
Fig. 2. 68%, 90% and 99% confidence contours for two parameters of interest; equivalent hydrogenic absorbing column (N_H) and spectral break energy, both in the observer frame. The dashed line represents the equivalent Hydrogen column density level of the Galaxy in the direction of B2 1308+326 (Dickey & Lockman, 1990).

Fig. 3. Rest-frame, νF_ν spectral energy distribution of B2 1308+326. The x-ray data has been corrected for absorption using the best-fit parameters (Table 2). The break at 2.8×10^{17} Hz is clearly seen in the middle of the x-ray data. Data contemporaneous with the ASCA observation are plotted in black. Non-simultaneous data are plotted in grey. Archive data are from NED[1]. Two parabolic fits to the synchrotron component are plotted, the black one is the best fit parabola to the contemporaneous data below the break, the grey parabola is a fit to the highest archival flux values in each band (from NED) and the ROSAT data below the break. The shift in frequency of the synchrotron peak is apparent.

2000; Sambruna et al., 1996; Pian et al., 1996) The SED of B2 1308+326 shows the synchrotron component peaking between 10^{12} Hz and 10^{14} Hz with the inverse Compton emission dominating by $\sim 2.8 \times 10^{17}$ Hz. The parabolic fit to the contemporaneous data indicates that the peak synchrotron frequency is $\sim 10^{12}$ Hz (Fig. 3). Although no variation in the 0.5–2.4 keV spectra was detected between the observations made with ROSAT and ASCA, examining the SED (Fig. 3) leads to the conclusion that the ROSAT synchrotron flux is incompatible with the radio and optical data obtained contemporaneously with ASCA. The effect of the absence of the synchrotron flux on the R1 spectrum was quantified by extrapolating the best-fit ROSAT synchrotron power-law past the spectral break to 2.4 keV. The 0.5–2.4 keV flux of this synchrotron power-law alone was subtracted from the composite synchrotron-IC R1 0.5–2.4 keV flux. The resulting (IC) flux was still fully consistent with the ASCA 0.5–2.4 keV flux. This indicates that the synchrotron-IC break occurred at lower energies during the ASCA observation than during R1 and that the ASCA spectrum is almost entirely dominated by an IC component that has not varied substantially at these energies despite the large change in the synchrotron flux. Chiaberge & Ghisellini (1999) have modelled synchrotron–self-Compton emission in blazars and successfully reproduced the SED of Mkn 421 in different flux states (Macomb et al., 1995). Their model allows a peak synchrotron variation of nearly two orders of magnitude that leaves the low-frequency end of the IC component largely unaffected, consistent with the SED observed here and in Mkn 421 (Macomb et al., 1995). Major variability of the IC component would however be expected at γ-ray energies because of the large change in the synchrotron emission. Observations at γ-ray energies can strongly constrain synchrotron-IC models (Maraschi et al., 1999). A parabolic fit to the highest archival fluxes in each

waveband and the ROSAT data below the spectral break yields a peak synchrotron frequency of $\sim 10^{14}$ Hz. This indicates that the peak synchrotron frequency of B2 1308+326 may decrease with flux, an important indicator in deciding the nature of the inverse Compton emission in this source (Böttcher, 1999). This type of spectral break and the possibility of increasing synchrotron peak frequency with increasing flux have also been observed with *BeppoSAX* in the blazar S5 0716+714 (Giommi et al., 1999).

The ASCA lightcurve yields no evidence for variability above 7.5×10^{-14} erg cm^{-2} s^{-1} on timescales of hours. V-band optical photometry from both Calar Alto observations yields a magnitude of 18.3 ± 0.25. A limit on the variability of the source of 0.08 mag. was found using differential photometry. Therefore, no constraints can be placed on the superluminal gravitational lensing scenario in this AGN because of the absence of variability.

The optical spectrum (Fig. 4) observed on 16 June 1996 is intermediate between the extreme spectra previously observed

---

[1] The NASA/IPAC Extragalactic Database (NED) is operated by the Jet Propulsion Laboratory, California Institute of Technology, under contract with the National Aeronautics and Space Administration.
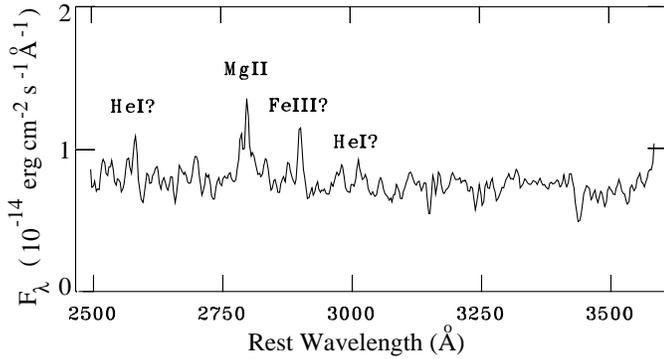
Fig. 4. Redshift ($z = 0.997$) corrected optical spectrum. The absolute flux calibration is unreliable due to non-photometric conditions during the observation, but is included for completeness. The Mg II emission feature is identified.

(Miller et al., 1978; Stickel et al., 1993). The equivalent width of the Mg II line was ~15 Å. The absolute flux calibration for this spectrum is unreliable due to non-photometric conditions during the observation; it was therefore not possible to obtain a continuum level or line fluxes from the ASCA observations.

The results of the radio observations (Fig. 5) over 20 years indicate that B2 1308+326 was in an intermediate radio flux state during these observations.

5. Discussion

Although BL Lacs were originally classified as XBLs or RBLs depending on the energy band in which they were first discovered, recent work has focused on determining the physical distinctions between the two types (Padovani & Giommi, 1995; Fossati et al., 1997; Georganopoulos & Marscher, 1998b) and their relation to the other subclass of blazar, FSRQs (Sambruna et al., 2000; Sambruna, 1997; Fossati et al., 1998; Ghisellini et al., 1998). The spectral energy distributions of XBLs and RBLs differ markedly, with the peak in synchrotron output generally occurring in the x-ray range for the former and the infrared range for the latter (Padovani & Giommi, 1995). This property has allowed BL Lacs to be classified as low-frequency peaked BL Lacs (LBLs, roughly the same sample as RBLs) and high-frequency peaked BL Lacs (HBLs, approximate to XBLs). Such differences may arise due to changes in the dominant radiation mechanism occurring as a function of both the angle between the line of sight and the bulk velocity (Ghisellini & Maraschi, 1989), although it has been demonstrated, assuming certain conditions, that the complete range of properties observed in blazars are difficult to account for solely by a change in orientation of the jet (Sambruna et al., 1996). On the other hand, XBLs and RBLs have different variability timescales, a fact that is very naturally explained with the orientation hypothesis (Heidt & Wagner, 1998). The recent RGB sample revealed BL Lacs intermediate between XBLs and RBLs, indicating that there is no bi-modal distribution in BL Lacs and that they span peak synchrotron frequencies continuously from IR to x-ray wavelengths (Laurent-Muehleisen et al., 1999).
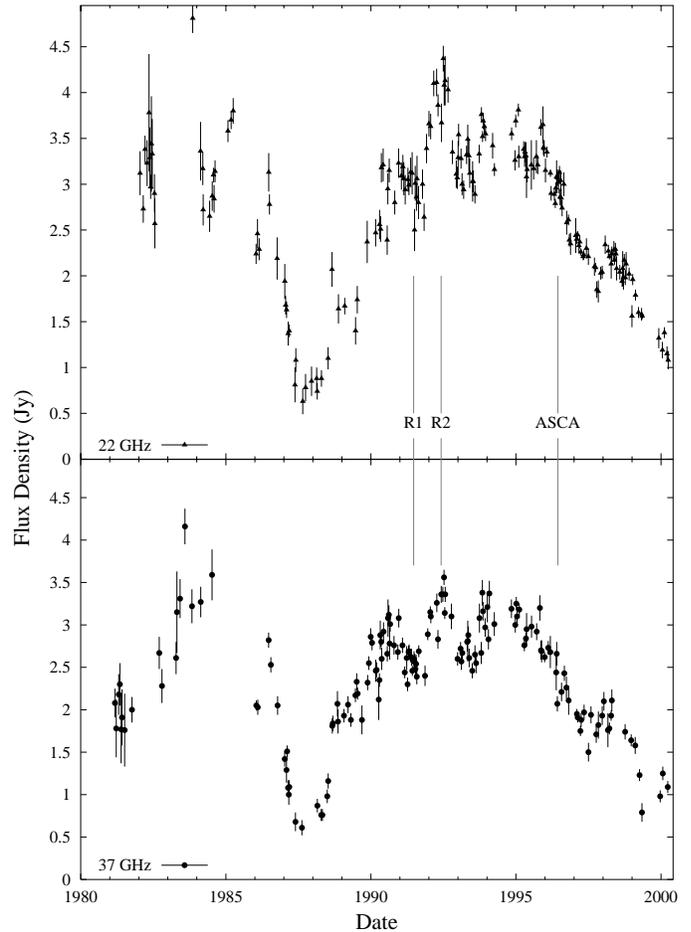
Fig. 5. 1980–2000 radio lightcurve at 22 GHz (top) and 37 GHz (bottom) obtained at the Metsähovi Radio Observatory. The times of the ASCA and ROSAT (R1 and R2) observations are indicated.

One hypothesis connecting FSRQs and BL Lacs is that they are high and low luminosity radio galaxies respectively that are highly-relativistically beamed towards the observer (Padovani, 1992). A more recent theory connects FSRQs, LBLs and HBLs in a sequence of increasing peak synchrotron frequencies and decreasing bolometric luminosity (Fossati et al., 1998; Sambruna et al., 2000); however, roughly 25% of FSRQs in the Deep X-ray Radio Blazar Survey (Perlman et al., 1998) have HBL-like radio–x-ray broadband spectral indices (α_{RX}), indicating that the synchrotron peak frequencies (ν_{peak}) for FSRQs reach energies at least as high as those of HBLs, since α_{RX} is strongly correlated with ν_{peak} (Fossati et al., 1998, and references therein). In this theory, blazars with strong thermal emission or strong emission lines (FSRQs) should have soft x-ray spectra dominated by inverse Compton (IC) emission produced by jet electrons scattering photons produced externally to the jet (external Compton, EC model). Blazars with intrinsically weak emission lines (BL Lacs) are expected to have their IC component dominated by jet electrons scattering photons produced in the jet via synchrotron emission (synchrotron self-Compton, SSC model). Böttcher (1999) has postulated that EC-dominated spectra have peak synchrotron frequencies that decrease with in-

creases in flux. The peak synchrotron frequency of B2 1308+326 appears to decrease with decreasing flux. While this synchrotron peak shift behaviour is contrary to the trend found in samples of blazars (Kubo et al., 1998; Fossati et al., 1998) it is not at all unusual in flares detected in individual sources (e.g. Catanese et al. 1997). Without IR photometry it is not possible to determine precisely the peak synchrotron frequency at the time of these observations. The optical observations were obtained simultaneous with, and two weeks after, the ASCA observations and yielded compatible results on both occasions. The radio data nearest the ASCA observations were taken on 4 June 1996 at 37 GHz, and on 5 and 20 June 1996 at 22 GHz. The radio variability during the surrounding months was less than 30%. The spectrum would have to deviate significantly from a parabolic shape in order to peak above 10^{14} Hz and still manage to drop as low as 18.3 mag. in the optical. Such a spectral shape cannot be ruled out without accurate modelling of the synchrotron component, however it is very likely that the synchrotron peak did occur below 10^{14} Hz in the faint state observed here, indicating that the synchrotron peak frequency decreases with decreasing flux and that SSC is the more likely emission mechanism in this blazar (Böttcher, 1999). Simultaneous GeV observations are required to determine if there is excess IC emission resulting from the EC component. Such observations would be useful for testing the model proposed for PKS 0548+134 (Mukherjee et al., 1999) and the trend detected by Kubo et al. (1998) in a sample of 18 blazars.

The dominance of the IC component in B2 1308+326 above 2.8×10^{17} Hz is evident from Fig. 3. The relatively low energy of this break is consistent with expectations of LBLs (Giommi et al., 1995), but somewhat exceeds expectations for FSRQs in the blazar paradigm described by Sambruna et al. (2000). The contemporaneous nature of the observations rules out distortion of the spectrum due to source variability.

The primary reason for classifying B2 1308+326 as a BL Lac rather than a FSRQ is its largely featureless optical continuum which is one of the defining features of the BL Lac class, with rest-frame $W_\lambda < 5$ Å for any line (Sambruna et al., 1996). This criterion has been justifiably criticised as arbitrary (Kollgaard et al., 1992; Marchã et al., 1996; Scarpa & Falomo, 1997) partly on the basis that some sources (such as B2 1308+326) have W_λ that vary substantially across this boundary. Nevertheless, weak or absent emission lines is a distinguishing property of these sources (Padovani, 1992). The rest-frame W_λ of the Mg II line in B2 1308+326 detected by Miller et al. (1978) was < 5 Å and no lines were observed by Wills & Wills (1979). However, an Mg II $W_\lambda = 18.6$ Å in the rest-frame was observed in March 1989 by Stickel et al. (1993) in a very low luminosity state $m_R = 19.0$ mag ($AB_{5500Å} \sim 18.5$ mag from the spectrum), comparable in brightness to the observations presented here. The W_λ (~ 15 Å) reported in this paper and by Stickel et al. (1993) place B2 1308+326 outside the traditional limits for BL Lacs, while previous observations place it well inside.

The level of the continuum may be the most significant factor in changing the value of W_λ for the Mg II line and not variation

Table 4. Average radio, optical and x-ray luminosities for samples of XBLs (Slew), RBLs (1 Jy) and FSRQs. The Slew, 1 Jy and FSRQ sample data (Cols. 1, 2 and 3 respectively) are from Fossati et al. (1998). Luminosities calculated from the contemporaneous data for B2 1308+326 are shown for comparison. The 5 GHz luminosity of B2 1308+326 is estimated from an extrapolation of the best-fit parabola to the contemporaneous data. The minimum recorded flux at 5 GHz and the maximum recorded flux in the V-band for B2 1308+326 are shown in parentheses. Luminosities are given in units of erg s^{-1}.

Band	XBLs (Slew)	RBLs (1 Jy)	FSRQ	B2 1308+326
5 GHz	41.71	43.69	44.81	45.4 (44.0)
V-band	44.91	45.68	46.58	45.1 (46.7)
1 keV	44.94	44.72	45.98	44.9

of the intrinsic line luminosity, since (a) both large W_λ measurements were made near low luminosity states and (b) the line flux of 3.8×10^{-15} erg cm^{-2} s^{-1} reported by Miller et al. (1978) is within a factor of two of the value of 5.8×10^{-15} erg cm^{-2} s^{-1} of Stickel et al. (1993) even though W_λ differs substantially between the observations. No error was given for these measurements. Padovani (1992) has shown that in general the low values of W_λ observed in BL Lacs are due to intrinsically less luminous line fluxes than in quasars. Sambruna et al. (2000) find Mg II luminosities of $L_{Mg II} \sim (4–40) \times 10^{43}$ erg s^{-1} for a sample of three FSRQs, comparable to but higher than B2 1308+326, with $L_{Mg II} = 1.5 \times 10^{43}$ erg s^{-1}. It therefore appears that the small values of W_λ observed in B2 1308+326 are due mostly to the extremely bright continuum. Unfortunately, it was not possible to obtain a line flux from these observations. Similar intermediate BL Lac–QSO behaviour is not unique to B2 1308+326, and has also been observed in PKS 0521-365 for example (Scarpa et al., 1999).

The existence of sources intermediate between BL Lac and QSOs is expected in the blazar unification paradigm presented by Fossati et al. (1998), where synchrotron peak frequency is correlated with source luminosity. X-ray, optical and radio luminosities for B2 1308+326 are compared to averages for the different blazar samples examined by Fossati et al. (1998) in Table 4. It is interesting to note that the luminosities for B2 1308+326 span the range between the RBL-FSRQ averages.

Sources intermediate between BL Lac and QSOs with luminous emission lines that are SSC-dominated and have high synchrotron peak frequencies (Perlman et al., 1998; Sambruna et al., 2000) still pose serious problems to the unification scheme proposed by Fossati et al. (1998). It has recently been pointed out (Georganopoulos, 2000) that the observed differences between FSRQs with high synchrotron peak frequencies ("blue quasars") and HBLs can be explained by taking into account the orientation of the jet as well as the intrinsic source luminosity. In a similar way earlier unification schemes have attempted to unify intrinsically lower luminosity FR I radio galaxies with BL Lacs and the higher luminosity FR II radio galaxies with quasars (Padovani, 1992; Ghisellini et al., 1993). It now seems likely that quasars and BL Lacs form two distinct populations of

Table 5. Comparison of relativistic jet parameters calculated using contemporaneous data compared to those of Ghisellini et al. (1993) and Teräsranta & Valtaoja (1994). F_m is the flux at the synchrotron self-absorption frequency ν_m, F_x is the x-ray or optical flux at the energy ν_x, ν_b is the synchrotron high energy cut-off frequency, α is the spectral index of the thin synchrotron emission, β_a is the highest superluminal speed, θ_d is the VLBI FWHM core size at ν_m, z is the source redshift, δ is a lower limit on the Doppler boost factor, T_B is the observed brightness temperature, ϕ is an upper limit on the angle between the jet velocity and the line of sight and Γ is a lower limit on the Lorentz factor of the jet. δ, T_B, ϕ and Γ were calculated using the data listed in that row. The third and fourth rows use data from observations made contemporaneously with the ASCA observations using the two different VLBI core sizes reported by Gabuzda et al. (1993).

F_m (Jy)	ν_m (GHz)	F_x (Jy)	ν_x (keV)	ν_b (GHz)	α	β_a^{Ga}	θ_d (mas)	z	δ	T_B (10^{12} K)	ϕ (°)	Γ
1.97^{Gh}	5.0^{Gh}	0.3×10^{-6} ^{Gh}	1^{Gh}	1×10^{5} ^{Gh}	0.75^{Gh}	15.75	0.5^{Gh}	0.996^{Gh}	6.8^{Gh}	1.11^{Gh}	6.1	21.7
–	–	–	–	–	–	15.75	–	0.992^{T}	1.9^{T}	6.40^{T}	7.2	68.0
1.22^{Ga}	5.0^{Ga}	0.18×10^{-3}	2.28×10^{-3}	1×10^{3}	0.80	15.75	0.05^{Ga}	0.997	122	69.0	0.12	62.0
0.76^{Ga}	5.0^{Ga}	0.18×10^{-3}	2.28×10^{-3}	1×10^{3}	0.80	15.75	0.18^{Ga}	0.997	9.4	3.35	5.37	18.0

^{Gh} Data from Ghisellini et al. (1993)
^{Ga} Data from Gabuzda et al. (1993)
^{T} Data from Teräsranta & Valtaoja (1994)

higher and lower luminosity AGN respectively, where the orientation of the jet influences the luminosity and peak synchrotron frequency. The unusual intermediate properties of B2 1308+326 make it an ideal candidate for studying the overlap between the BL Lac and QSO categories. It may therefore represent the prototype of this kind of composite source.

5.1. Gravitational microlensing

The gravitational microlensing scenario (Gabuzda et al., 1993; McBreen & Metcalfe, 1987), provides an alternate explanation for the BL Lac properties of B2 1308+326. Its high bolometric luminosity is comparable to that of other gravitationally lensed candidates AO 0235+164 (Rabbette et al., 1996) and PKS 0537-441 (Romero et al., 1999; Perlman et al., 1996) and may be due to amplification by a foreground galaxy. Mg II absorption lines with very small W_λ (~ 0.4 Å) were reported (Miller et al., 1978) at $z = 0.879$ in B2 1308+326. These lines have not been confirmed by later observations. Recent imaging with HST (Urry et al., 1999) did not confirm the detection of spatially extended emission (Stickel et al., 1993) and no evidence was found for a foreground lensing galaxy. Such a galaxy is therefore limited to an I-band magnitude greater than 20.1, which, if the galaxy were at a redshift $z = 0.879$ implies $M_I \gtrsim -23$, thus not constraining its luminosity significantly. The absorbing column towards B2 1308+326 is greater than that expected from our Galaxy (Fig. 2). The excess absorption could be due to an absorber at $z < 0.997$ or equally, to absorption in the host galaxy of B2 1308+326. The detection of excess absorption therefore does not exclude the possibility of a foreground lensing galaxy. A more detailed spectroscopic observation with XMM could determine the redshift of the foreground absorber. Sensitive, high-resolution optical spectroscopy could confirm the detection of Mg II absorption lines (Miller et al., 1978) and thus also determine the redshift of such an absorber.

5.2. Constraints on beaming in B2 1308+326

Contemporaneous multiwavelength observations allow the determination of a lower limit on the doppler boost factor (δ), the corresponding observed brightness temperature T_B, the maximum angle (ϕ) between the line of sight and the velocity of the relativistic jet as well as the minimum Lorentz factor of the jet, Γ. Ghisellini et al. (1993) have derived these values for B2 1308+326 with data from different epochs, using the equations:

$$\delta = (1+z) f(\alpha) F_m \left(\frac{\ln (\nu_b/\nu_m)}{F_x \theta_d^{6+4\alpha} \nu_x^\alpha \nu_m^{5+3\alpha}} \right)^{\frac{1}{4+2\alpha}} \quad (1)$$

$$T_B = 1.77 \times 10^{12} (1+z) \frac{F_m}{\theta_d^2 \nu_m^2} \, \text{K} \quad (2)$$

$$\phi = \arctan \frac{2\beta_a}{\beta_a^2 + \delta^2 - 1} \quad (3)$$

and

$$\Gamma = \frac{\beta_a^2 + \delta^2 + 1}{2\delta}, \quad (4)$$

where F_m and F_x are the fluxes in Jy at the synchrotron self-absorption frequency, ν_m (GHz), and at the x-ray or optical energy, ν_x (keV) respectively; ν_b is the synchrotron high energy cut-off frequency; α is the spectral index of the thin synchrotron emission defined from $F_\nu \propto \nu^{-\alpha}$; β_a is the fastest reported apparent superluminal speed; θ_d is the VLBI FWHM core size (Marscher, 1977) in milliarcseconds (mas) at ν_m; z is the redshift of the source. A comparison of these values obtained at different epochs for b2 1308+326 is made in Table 5.

It has been noted that the largest source of error in Eq. (1) is the determination of the VLBI core size, θ_d (Madau et al., 1987). This value is crucial in determining the limit on δ.

Ghisellini et al. (1993) calculate $\delta = 6.8$ using $\theta_d = 0.5$ mas at 5 GHz. High resolution VLBI images of B2 1308+326 were presented by Gabuzda et al. (1993) obtained in 1987 and 1989.

Using the 5 GHz fluxes and corresponding FWHM core sizes of Gabuzda et al. (1993), δ values of 122 and 9.4 were determined with the data presented here. Clearly the core size is variable and further constraints on δ would require VLBI imaging simultaneous with observations at other wavelengths.

Teräsranta & Valtaoja (1994) use the radio variability timescales of B2 1308+326 to deduce a lower limit for the doppler boost factor of $\delta = 1.9$ and the corresponding maximum observed brightness temperature $T_{B,max} = 6.4 \times 10^{12}$ K. The 22 GHz light curve used for this calculation is plotted in Fig. 5. This method provides a useful independent measure of δ. A comparison of these values with those derived using Eqs. (1)–(4) are given in Table 5. Two sets of values have been derived with the data obtained contemporaneously with ASCA using the different core sizes reported by Gabuzda et al. (1993). The contemporaneous data indicates that the synchrotron peak frequency is roughly 10^{12} Hz (Fig. 3) and this value was used for ν_b. A similar fit to the highest archival fluxes in each waveband and the ROSAT data below the spectral break yields a peak synchrotron frequency of $\sim 10^{14}$ Hz. The V-band flux and frequency were used instead of the 1 keV flux in these calculations, as the 1 keV flux at the time of these observations was almost certainly dominated by inverse Compton emission.

Three of the limits on δ agree within a factor of five (Table 5). The extreme value of $\delta = 122$, obtained using the core size $\theta_d = 0.05$ mas, is unlikely given the low flux state of the source during these observations. While the upper limits on ϕ are consistent with expected jet angles for RBLs, they are also consistent with those of highly-polarised quasars (HPQs; Ghisellini et al. 1993, Urry & Padovani 1995). Quasars generally appear to have larger values of δ than BL Lacs (Gabuzda et al., 1993; Teräsranta & Valtaoja, 1994). A mean δ of 8.3 for HPQs and 1.3 for BL Lacs (Gabuzda et al., 1993) indicates that B2 1308+326 with $\delta = 9.4$, is rather extreme for a typical BL Lac.

6. Conclusions

The blazar B2 1308+326 was observed contemporaneously at x-ray, optical and radio wavelengths in June 1996. The source was in a low synchrotron flux state at the time of observation and no variability was detected. The ROSAT data reveal an x-ray spectrum that is best fit by a broken power law with absorber model, with the break at 1.1 keV in the rest-frame of the blazar. The break is probably due to the emerging dominance of the IC over the synchrotron component. The frequency of the peak synchrotron emission component appears to have decreased with decreasing flux, thus indicating that SSC may be the dominant emission mechanism in this source. The x-ray IC component is unaffected by the large change in the synchrotron emission. Mg II emission was observed with rest $W_\lambda \sim 15$ Å, significantly different from the W_λ values previously reported. The variable W_λ emission in B2 1308+326 is probably mostly due to the highly variable continuum. Although values of W_λ are quite small, the line luminosity is only slightly lower than in a sample of QHBs. A lower limit on the Doppler boost factor obtained from the contemporaneous data is consistent with

expectations for HPQs but is higher than expected for BL Lacs. X-ray absorption at a level in excess of the Galactic value was detected and indicates the possible presence of a foreground absorber.

B2 1308+326 is a typical RBL in terms of peak synchrotron power and optical variability, but with a very large bolometric luminosity, variable line emission and a high Doppler boost factor also has quasar-like attributes. It may be an intermediate or transitional AGN or a gravitationally microlensed quasar, given its absorption above the Galactic level. Future x-ray observations could determine the nature of the absorber. Further simultaneous multiwavelength observations of this possibly prototypical intermediate blazar could determine the cause of both its BL Lac and its quasar-like properties, providing insight into the relation between BL Lacs and FSRQs.

References

Angel J.R.P., Stockman H.S., 1980, ARA&A 18, 321
Bevington P.R., Robinson D.K., 1992, In: Data reduction and error analysis for the physical sciences. 2nd ed., McGraw-Hill, New York
Böttcher M., 1999, ApJ 515, L21
Brown L.M.J., Robson E.I., Gear W.K., et al., 1989, ApJ 340, 129
Catanese M., Bradbury S.M., Breslin A.C., et al., 1997, ApJ 487, L143
Chiaberge M., Ghisellini G., 1999, MNRAS 306, 551
Comastri A., Molendi S., Ghisellini G., 1995, MNRAS 277, 297
Costamante L., Ghisellini G., Giommi P., et al., 2000, astro-ph/0001410
Dickey J.M., Lockman F.J., 1990, ARA&A 28, 215
Fanaroff B.L., Riley J.M., 1974, MNRAS 167, 31p
Fiorucci M., Tosti G., Rizzi N., 1998, PASP 110, 105
Fossati G., Celotti A., Ghisellini G., Maraschi L., 1997, MNRAS 289, 136
Fossati G., Maraschi L., Celotti A., Comastri A., Ghisellini G., 1998, MNRAS 299, 433
Fossati G., Celotti A., Chiaberge M., et al., 2000, astro-ph/0005066
Gabuzda D.C., Kollgaard R.I., Roberts D.H., Wardle J.F.C., 1993, ApJ 410, 39
Georganopoulos M., 2000, astro-ph/0008482
Georganopoulos M., Marscher A.P., 1998a, ApJ 506, L11
Georganopoulos M., Marscher A.P., 1998b, ApJ 506, 621
Ghisellini G., Maraschi L., 1989, ApJ 340, 181
Ghisellini G., Padovani P., Celotti A., Maraschi L., 1993, ApJ 407, 65
Ghisellini G., Celotti A., Fossati G., Maraschi L., Comastri A., 1998, MNRAS 301, 451
Giommi P., Ansari S.G., Micol A., 1995, A&AS 109, 267
Giommi P., Massaro E., Chiappetti L., et al., 1999, A&A 351, 59
Gopal-Krishna, Subramanian K., 1991, Nat 349, 766
Heidt J., Wagner S.J., 1998, A&A 329, 853
Inoue H., 1993, Experimental Astronomy (ISSN 0922-6435) 4, 1
Iwasawa K., Fabian A.C., Nandra K., 1999, MNRAS 307, 611
Kollgaard R.I., Wardle J.F.C., Roberts D.H., 1990, AJ 100, 1057
Kollgaard R.I., Wardle J.F.C., Roberts D.H., Gabuzda D.C., 1992, AJ 104, 1687
Kollgaard R.I., Gabuzda D.C., Feigelson E.D., 1996, ApJ 460, 174
Kubo H., Takahashi T., Madejski G., et al., 1998, ApJ 504, 693

Lamer G., Brunner H., Staubert R., 1996, A&A 311, 384

Laurent-Muehleisen S.A., Kollgaard R.I., Feigelson E.D., Brinkmann W., Siebert J., 1999, ApJ 525, 127

Macomb D.J., Akerlof C.W., Aller H.D., et al., 1995, ApJ 449, L99

Madau P., Ghisellini G., Persic M., 1987, MNRAS 224, 257

Maraschi L., Fossati G., Tavecchio F., et al., 1999, ApJ 526, L81

Marchã M.J.M., Browne I.W.A., Impey C.D., Smith P.S., 1996, MNRAS 281, 425

Marscher A.P., 1977, ApJ 216, 244

McBreen B., Metcalfe L., 1987, Nat 330, 348

Miller J.S., French H.B., Hawley S.A., 1978, In: A.M. Wolfe (ed.) Pittsburgh Conference on BL Lac Objects, University of Pittsburgh, Pittsburgh, p. 176

Morrison R., McCammon D., 1983, ApJ 270, 119

Mufson S.L., Stein W.A., Wisniewski W.Z., et al., 1985, ApJ 288, 718

Mukherjee R., Böttcher M., Hartman R.C., et al., 1999, ApJ 527, 132

Nottale L., 1986, A&A 157, 383

Ostriker J.P., Vietri M., 1990, Nat 344, 45

Padovani P., 1992, MNRAS 257, 404

Padovani P., Giommi P., 1995, ApJ 444, 567

Perlman E.S., Stocke J.T., Schachter J.F., et al., 1996, ApJS 104, 251

Perlman E.S., Padovani P., Giommi P., et al., 1998, AJ 115, 1253

Pfeffermann E., Briel U.G., 1986, Proceedings of SPIE 597, 208

Pian E., Falomo R., Ghisellini G., et al., 1996, ApJ 459, 169

Pian E., Vacanti G., Tagliaferri G., et al., 1998, ApJ 492, L17

Rabbette M., McBreen B., Steel S., Smith N., 1996, A&A 310, 1

Rabbette M., McBreen B., Smith N., Steel S., 1998, A&AS 129, 445

Romero G.E., Cellone S.A., Combi J.A., 1999, A&AS 135, 477

Sambruna R.M., 1997, ApJ 487, 536

Sambruna R.M., Maraschi L., Urry C.M., 1996, ApJ 463, 444

Sambruna R.M., Ghisellini G., Hooper E., et al., 1999, ApJ 515, 140

Sambruna R.M., Chou L.L., Urry C.M., 2000, ApJ 533, 650

Scarpa R., Falomo R., 1997, A&A 325, 109

Scarpa R., Urry C.M., Falomo R., Treves A., 1999, ApJ 526, 643

Stickel M., Fried J.W., Kühr H., Padovani P., Urry C.M., 1991, ApJ 374, 431

Stickel M., Fried J.W., Kühr H., 1993, A&AS 98, 393

Tanaka Y., Inoue H., Holt S.S., 1994, PASJ 46, L37

Teräsranta H., Valtaoja E., 1994, A&A 283, 51

Teräsranta H., Tornikoski M., Mujunen A., et al., 1998, A&AS 132, 305

Urry C.M., Padovani P., 1995, PASP 107, 803

Urry C.M., Falomo R., Scarpa R., et al., 1999, ApJ 512, 88

Urry C.M., Scarpa R., O'Dowd M., et al., 2000, ApJ 532, 816

Watson D., Hanlon L., McBreen B., et al., 1999, A&A 345, 414

Wills B.J., Wills D., 1979, ApJ 41, 689